

REPORTS

locene features that have expanded and contracted in concert with the large-scale warming and cooling phases of the Holocene in Africa. The ice core records from the SIF and FWG indicate that ice cover on Africa's highest mountain has varied through the Holocene. The FWG appears to have formed only in the past few centuries, likely at the onset of the coldest part of the most recent Neoglacial or Little Ice Age period. We speculate that the FWG is an ephemeral feature, unlike the larger rim ice fields that have been more persistent through time.

Model-derived dates, coupled with ^{14}C ages for the bottom ice in the NIF, suggest that it began to grow ~ 11.7 ka and expanded during the African Humid Period. Clearly there was less ice on the summit of Kilimanjaro at ~ 4 ka, coincident with the "First Dark Age," the period of the greatest historically recorded drought in tropical Africa, which apparently extended to the Middle East and western Asia. The disappearance of Kilimanjaro's ice fields, expected between 2015 and 2020, will be unprecedented for the Holocene. This will be even more remarkable given that the NIF persisted through a severe ~ 300 -year drought that so disrupted the course of human endeavors that it is detectable from the historical and archaeological records throughout many areas of the world. A comparison of the chemical and physical properties preserved in the NIF with those in the water-saturated, rapidly shrinking FWG (36), coupled with the lack of melt features in the NIF and SIF cores, confirms that conditions similar to those of today have not existed in the past 11 millennia. The loss of Kilimanjaro's permanent ice fields will have both climatological and hydrological implications for local populations, who depend on the water generated from the ice fields during the dry seasons and monsoon failures.

References and Notes

- Equipment description and data are available at www.geo.umass.edu/climate/kibo.html.
- S. E. Nicholson, in *The Limnology, Climatology and Paleoclimatology of the East African Lakes*, T. C. Johnson, E. O. Odada, Eds. (Gordon and Breach, Amsterdam, 1996), pp. 25–56.
- S. Hastenrath, L. Greischar, *J. Glaciol.* **43**, 455 (1997).
- B. Messerli, *IAHS-AISH Publ.* **126**, 197 (1980).
- The 11 GPS positions were obtained from three different sources: two points of geodetic (cm) accuracy from a joint Tanzanian-German survey in September 1999 (37), seven points with accuracies of 2 to 5 m from surveys by D.R.H. and colleagues in February and June 2001, and two points of low accuracy (15 to 20 m) established by the Ohio State University (OSU) field party in February 2000, all weighted accordingly.
- M. W. Carter, A. A. Moghissi, *Health Phys.* **33**, 55 (1977).
- D. Palliard, L. Labeyrie, P. Yiou, *EOS* **77**, 379 (1996).
- J. F. Nye, *J. Glaciol.* **4**, 785 (1963).
- W. Dansgaard, S. J. Johnsen, *J. Glaciol.* **8**, 215 (1969).
- D. Verschuren, K. R. Laird, B. F. Cumming, *Nature* **403**, 410 (2000).
- M. Stuvier, P. J. Reimer, T. F. Braziunas, *Radiocarbon* **40**, 1127 (1998).
- L. G. Thompson et al., *Science* **282**, 1858 (1998).
- M. Bar-Matthews, A. Ayalon, A. Kaufman, G. J. Wasserburg, *Earth Planet. Sci. Lett.* **6**, 85 (1999).
- F. A. Street, A. T. Grove, *Quat. Res.* **12**, 83 (1976).
- S. E. Nicholson, H. Flohn, *Clim. Change* **2**, 313 (1980).
- J. E. Kutzbach, F. A. Street-Perrott, *Nature* **317**, 130 (1985).
- F. A. Street-Perrott, R. A. Perrott, *Nature* **343**, 607 (1990).
- A. T. Grove, A. Warren, *Geogr. J.* **134**, 194 (1968).
- A. Broström et al., *Geophys. Res. Lett.* **25**, 3615 (1998).
- C. Hillaire-Marcel, J. Casanova, *Palaeogeogr. Palaeoclimatol. Palaeocol.* **58**, 155 (1987).
- J. E. Kutzbach, *Quat. Res.* **14**, 210 (1980).
- L. G. Thompson, E. Mosley-Thompson, K. A. Henderson, *J. Quat. Sci.* **15**, 377 (2000).
- T. Blunier, J. Chappellaz, J. Schwander, B. Stauffer, D. Raynaud, *Nature* **374**, 46 (1995).
- R. B. Alley et al., *Geology* **25**, 483 (1997).
- P. Kilham, R. E. Hecky, *Limnol. Oceanogr.* **18**, 932 (1973).
- J. T. Nanyaro, U. Aswathanarayana, J. S. Mungure, *J. Afr. Earth Sci.* **2**, 129 (1984).
- S. J. Gaciri, T. C. Davies, *J. Hydrol.* **143**, 395 (1993).
- F. Sirocko et al., *Nature* **364**, 322 (1993).
- F. A. Street-Perrott, J. F. B. Mitchell, D. S. Marchant, J. S. Brunner, *Trans. R. Soc. Edinburgh Earth Sci.* **81**, 407 (1990).
- A. M. Swain, J. E. Kutzbach, S. Hastenrath, *Quat. Res.* **19**, 17 (1983).
- H. Weiss, in *Environmental Disaster and the Archeology of Human Response*, G. Bawden, R. M. Reycraft, Eds. (Anthropological Papers, No. 7, Maxwell Museum of Anthropology, University of New Mexico, Albuquerque, 2001), pp. 75–95.
- H.-J. Pachur, P. Hoelzmann, *J. Afr. Earth Sci.* **30**, 929 (2000).
- F. Gasse, E. Van Campo, *Earth Planet. Sci. Lett.* **126**, 435 (1994).
- H. N. Dalfes, G. Kukla, H. Wiess, *Third Millennium BC Climate Change and Old World Collapse* (NATO ASI Series I: Global Environmental Change, vol. 49, Springer, Berlin, 1994).
- H. M. Cullen et al., *Geology* **28**, 379 (2000).
- The ion concentrations from the water-saturated FWG (~ 1670 to 1920 A.D.) were compared with those measured in the NIF cores for the same time interval to support our contention that the NIF has not been water-saturated (measurements of FWG versus NIF, all in ppb: F^- , 3.3 versus 5.8; NO_3^- , 59.6 versus 255.5; SO_4^{2-} , 22.1 versus 69.4; Na^+ , 31.6 versus 126.8; K^+ , 8.9 versus 38.2; Mg^{2+} , 1.5 versus 4.9; and Ca^{2+} , 8.2 versus 42.1).
- J. Saburi et al., *Survey Rev.* **35**, 278 (2000).
- This project was funded by grant ATM-9910172 from the NSF's Earth System History Program. We thank M. Illner of the Geodetic Institute of the University of Karlsruhe (GIK) for providing positions and helping to locate the points of the survey carried out by a party with participants from GIK; Karlsruhe University of Applied Science; University College of Lands and Architectural Studies; the Surveys and Mapping Division, Tanzania; and Leica Geosystems. We thank R. Fox, International Library Manager, U.K. Ordnance Survey, for his help in searching for existing old photography and ground control points. Photomap (Kenya) Ltd. did an excellent job of taking our February 2000 aerial photographs. The Accelerator Mass Spectrometry (AMS) ^{14}C dates were measured by T. Guilderson of The University of California's Lawrence Livermore National Laboratory and by the National Ocean Sciences AMS Facility at Woods Hole Oceanographic Institution. We thank P. R. Edwards for the analytical chemistry measurements he made on NIF3 while he was a Byrd Postdoctoral Fellow. We are indebted to P. Ndesamburo and the staff of the Key's Hotel who facilitated securing the many permits and making logistical arrangements in Tanzania and to J. Minja (chief guide) and the 92 porters who made this project possible. This is Byrd Polar Research Center contribution number 1264.

Supporting Online Material

www.sciencemag.org/cgi/content/full/298/5593/589/DC1

Supporting Text

Figs. S1 and S2

Tables S1 and S2

References and Notes

23 April 2002; accepted 3 September 2002

A Primordial Origin of the Laplace Relation Among the Galilean Satellites

S. J. Peale* and Man Hoi Lee

Understanding the origin of the orbital resonances of the Galilean satellites of Jupiter will constrain the longevity of the extensive volcanism on Io, may explain a liquid ocean on Europa, and may guide studies of the dissipative properties of stars and Jupiter-like planets. The differential migration of the newly formed Galilean satellites due to interactions with a circumjovian disk can lead to the primordial formation of the Laplace relation $n_1 - 3n_2 + 2n_3 = 0$, where the n_i are the mean orbital angular velocities of Io, Europa, and Ganymede, respectively. This contrasts with the formation of the resonances by differential expansion of the orbits from tidal torques from Jupiter.

The orbital resonances among the Galilean satellites of Jupiter have led to sustained dissipation of tidal energy to produce astounding volcanos on Io and, probably, to maintain a liquid

ocean on Europa. Understanding the origin of these resonances will constrain the history of the satellites and their formation scenarios. The two models proposed are an assembly of the resonances through differential tidal expansion of the orbits from tides raised on Jupiter (1, 2) and a primordial origin of unspecified assembly and subsequent evolution away from exact resonance (3, 4). Here we discuss a means of

Department of Physics, University of California, Santa Barbara, CA 93106, USA.

*To whom correspondence should be addressed. E-mail: peale@io.physics.ucsb.edu

assembling the resonances during the formation process in support of a primordial origin.

The currently observed orbital resonances at the 2:1 mean motion commensurabilities involving Io-Europa and Europa-Ganymede are such that the resonance variables $\theta_1 = \lambda_1 - 2\lambda_2 + \varpi_1$ and $\theta_3 = \lambda_2 - 2\lambda_3 + \varpi_2$ librate about 0° and $\theta_2 = \lambda_1 - 2\lambda_2 + \varpi_2$ librates about 180° , all with small amplitude. Here the λ_i are mean orbital longitudes and the ϖ_i are the longitudes of periapse numbered consecutively for Io, Europa, and Ganymede, respectively. The simultaneous libration of θ_2 and θ_3 means the Laplace angle $\theta_5 = \theta_2 - \theta_3 = \lambda_1 - 3\lambda_2 + 2\lambda_3 \approx 180^\circ$ with small libration amplitude, leading to $n_1 - 3n_2 + 2n_3 = 0$, where $n_i = \dot{\lambda}_i$ are the mean angular velocities with the dot indicating time differentiation. This last libration condition is called the Laplace relation because Laplace first understood its stability. The geometry is such that conjunctions of Io and Europa occur when Io is near the periapse of its orbit and Europa is near its apoapse, and conjunctions of Europa and Ganymede occur when Europa is near its periapse. Ganymede can be anywhere in its orbit at the conjunctions with Europa, because the resonance variable $\theta_4 = \lambda_2 - 2\lambda_3 + \varpi_3$ circulates through all angles. The existence of this group of resonances with small amplitudes of libration implies an assembly of originally random orbits by dissipative processes.

A currently popular means of resonance assembly is by differential orbital expansion due to gravitational tides raised on Jupiter, principally by Io, and damping of the libration amplitudes by tidal dissipation within the satellites, mostly in Io (1, 2). Io's orbit expands more rapidly than Europa's, and capture of Io and Europa into the 2:1 orbital resonances is certain for a reasonably wide range of initial orbital eccentricities. Continued orbital expansion tends to drive the pair deeper into the resonance (i.e., driving $n_1 - 2n_2$ to smaller values) and thereby to increase the orbital eccentricities. But dissipation of tidal energy within the satellites tends to decrease the eccentricities, so an equilibrium can be reached where the eccentricities and the ratio of the mean motions are almost constant as the pair of satellites moves out together locked in the resonances (1, 2). Europa eventually encounters the 2:1 mean motion commensurability with Ganymede, where capture into the Laplace relation as the resonance variable θ_3 is trapped into libration about 0° has a probability of about 0.9 (1). θ_4 is circulating because the free eccentricity (5) of Ganymede's orbit exceeds the relatively small forced eccentricity in the resonance (6). The librations are damped by the tidal dissipation in Io. Variations of this scenario have been proposed by Malhotra and colleagues (7-9). The creation of the Laplace relation by differential tidal expansion of the orbits depends on the dissipation function Q_j of

Jupiter being sufficiently small ($\sim 10^6$) for non-negligible expansion of the orbits to occur, and the maintenance of the current configuration in equilibrium would require an even smaller Q_j ($\sim 2 \times 10^4$).

Greenberg, motivated by the difficulty of accounting for a sufficiently small Q_j necessary for the tidal origin or equilibrium described above and the observed positive n_1 , proposed a primordial origin of the Laplace relation (3, 4). He described evolution from much deeper in the resonances (i.e., with $n_1 - 2n_2$ approaching zero and thereby forcing much larger orbital eccentricities). The path from deep resonance as dissipation decreased the eccentricities is characterized by stable librations of the resonance angles about centers much different from the 0° or 180° currently observed here. The high dissipation rates at the high eccentricities imply rapid decay of the resonances ($< 10^7$ year time scale), and the only way to preserve them for 4.6×10^9 years was to have a sufficiently low $Q_j \sim 10^6$ to allow at least an episodic heating and cooling of Io, albeit not as low as would be required by the equilibrium model. Now we would be observing the system on its way out of the resonance, which lowers the eccentricities and, hence, the heating rates. Eventually Io cools and the dissipation function Q_j of Io increases to the point at which the Jupiter torque "wins," pushing the system back to higher eccentricities to repeat the cycle (3, 10). It is not certain that Io could cool rapidly enough in this scenario, but $Q_j \sim 10^6$ could delay the evolution from deep resonance sufficiently to prevent its destruction (11). Major problems with this scenario were that (i) there was no mechanism for placing the system in the resonances at the time of satellite formation and (ii) evolution through the high-eccentricity phases could not be followed with the analytic theory. Here, we describe a mechanism that addresses both of these problems and adds support to Greenberg's hypothesis.

Constraints on the formation of the Galilean satellites of Jupiter have been established by theoretical analysis and the Galileo spacecraft observations. The nearly coplanar and nearly circular orbits of the four large satellites imply formation within a dissipative, equatorial disk of gas and solid particles formed, perhaps, by one of several processes during the formation of Jupiter (12). Ganymede and Callisto are about 50% ice and 50% rock by mass (13). Europa has a layer of water and ice 80 to 170 km thick (14). The large amount of relatively volatile material in Ganymede and Callisto implies that the disk temperature remained sufficiently cool during the accretion process that icy particles could persist. Callisto may not be fully differentiated (15, 16), a state that requires an accretion time scale $\sim 10^6$ years to keep interior temperatures below 273 K (17, 18).

Accretion models for the Galilean satellites have typically assumed an initial disk with suf-

ficient solid material to form the satellites and with gas added to bring the mixture up to solar composition—the so-called minimum mass sub nebula (MMSN) (12). But a careful evaluation of the processes in such a massive disk (19) indicate that temperatures would generally be too high and accretion rates too fast to allow formation of the satellites with their observed properties. In particular, it would be difficult if not impossible to keep Callisto only partially differentiated. Therefore, it is likely that the satellites formed near the end of Jupiter's formation when the flux of material into Jupiter through an accretion disk was greatly reduced (18). Theoretical calculations (20) show that Jupiter would limit this flux by opening a gap in the disk of material surrounding the Sun when the planet's mass approached its current value. Hydrodynamical simulations (21-24) show that gas and particles continue to trickle through the gap in two streams entering at the inner and outer Lagrange points to form an accretion disk around Jupiter. The surface mass density of the accretion disk resulting from this scenario is sufficiently less than the MMSN to allow the slow accumulation of the satellites in a cool environment.

By modeling processes in this disk, Canup and Ward (19) have found a scenario of satellite accretion that appears to satisfy all of the observational and theoretical constraints imposed by the satellites' current properties. The important characteristics of the model, for our purposes, are that the formation time scales of the individual Galilean satellites are similar and that the satellites migrate toward Jupiter while the disk persists. The migration is the result of the gravitational interaction of the satellites with spiral density waves generated in the disk material at mean motion commensurabilities with the satellites (Lindblad and corotation resonances). The satellites are not sufficiently massive to open gaps in the disk and, thus, they execute the so-called Type I drift (25), whose time scale is inversely proportional to both the disk surface mass density and the satellite mass.

The key ingredient of the Canup-Ward model that allows an alternative history of the Galilean satellite resonant system is that Ganymede's orbit converges on those of Europa and Io because of its faster Type I migration induced by its greater mass. Callisto is left behind because of its smaller mass. Various choices of the viscosity parameter α and opacity of the disk lead to many different migration rates for the satellites, but all reasonable choices lead to converging orbits of the inner three satellites [figs. 7c, 8c, and 9c of (19)] because of Ganymede's more rapid migration. Any other model of formation will also suffice for our purposes here, provided that the formation time scales of all the satellites are comparable and that the disk persists long enough for differential migration to lead to converging orbits (26).

REPORTS

We demonstrate (Fig. 1) that the Laplace relation can be established primordially during the final stages of satellite accretion by allowing Ganymede's orbit to migrate inward on the 10^5 year time scale of the Canup-Ward model (19), whereas Europa and Io initially migrate more slowly on a 2×10^5 year time scale. (The very rapid migration rates implied for disk densities corresponding to the MMSN would most likely preclude the capture of the satellites in any resonances during differential migration.) The satellites start in an initial configuration where the orbits are separated by distances greater than those appropriate to the 2:1 mean motion commensurability. The numerical calculations are done both by the Wisdom-Holman (27) symplectic integrator contained in the SWIFT package (28) and in a center-of-mass cartesian coordinate system with a Bulirsch-Stoer algorithm. The algorithms are modified as described in (29) to accommodate the migration and eccentricity damping, and both algorithms yield similar results. Europa is first captured into the 2:1 mean motion resonances with Ganymede and Io is subsequently picked up in the 2:1 resonances with Europa, simultaneously establishing the Laplace relation (30).

The orbital eccentricities of the satellites are damped by interactions with the gas disk [e.g., (31)] and eventually by tidal dissipation in the satellites [e.g., (2)]. In the case of disk interactions, the ratio of the inverse time scales is given by (31)

$$\frac{1/\tau_e}{1/\tau_a} = \frac{|\dot{e}/e|}{|\dot{a}/a|} = 9 \frac{C_e}{C_a} \left(\frac{H}{a}\right)^{-2} \approx 30 \quad (1)$$

where H/a is the ratio of the scale height of the disk H to the semimajor axis of the orbit a . $H/a \approx 0.1$ is assumed constant in the disk, where the numerical value follows from the conditions in the Canup-Ward model (19). $C_a \approx 3$ is the coefficient of the expression for \dot{a}/a (31, 32), and $C_e \approx 0.1$ is the coefficient in the expression for \dot{e}/e (31). For the integrations, we assumed that the time scales for migration in a and in eccentricity damping are constant and, hence, the ratio of the inverse time scales is fixed, with $|\dot{e}/e|/|\dot{a}/a| = 30$ from Eq. 1 assumed for all three satellites. The eccentricity damping causes the eccentricities to reach constant asymptotic values (Fig. 1), which are reduced if the ratio of the inverse time scales in Eq. 1 is increased. The evolution is reasonably independent of the rate of migration up to a certain point. An example where the satellite migration rates were 30 times larger led to a very similar evolution.

Although all of the resonance variables, including the Laplace angle θ_5 , are librating in the primordial configuration of the satellites (Fig. 1), the geometry of the system differs from the current configuration, where all resonance variables, except θ_4 , librate about either 0° or 180° , as described above. The centers of libration of θ_5 and θ_2 are near 80° instead of 180° and that

of θ_1 is near -30° instead of 0° (Fig. 2). θ_4 would normally librate about 180° for smaller eccentricities, but here it is near -10° . Only θ_3 has the same libration center near 0° that it has now. Conjunctions would no longer occur near the lines of apsides of the orbits. This is consistent with the locus of stable libration centers for θ_5 branching symmetrically from 180° as the system is driven deeper into the resonances than the current configuration (4). The occurrence of libration centers of both θ_2 and θ_5 near -80° in some of our calculations is verification of the symmetric branches.

As the satellites move closer to Jupiter and the disk dissipates, tidal dissipation in the satellites eventually dominates the eccentricity damping. At the same time, the dissipation of tidal energy in Jupiter from tides raised by the satellites results in the torques that tend to push the satellites outward, thereby tending to increase the eccentricities [e.g. (2)]. Because the current orbital eccentricities are smaller than the primordial asymptotic values (Fig. 1), the ten-

dency for the eccentricities to decrease due to dissipation in the satellites must dominate the effect of the tides raised on Jupiter that tend to increase the eccentricities—at least at the end of migration. The tidal time scale for eccentricity damping is $|e/\dot{e}| \approx 6.5 \times 10^4 Q_1/f$ years for Io, which is derived from expressions given in (33). Here $Q_1 \approx 30$ to 100 for rocky material and f is a factor to account for an inhomogeneous structure of Io, which can be as high as 13 for a two-layer model consisting of a solid mantle over a molten interior (34). The tidal time scale for eccentricity damping is probably more than 6 times as long as the migration time scale of the Canup-Ward model, and possibly 100 times as long as the disk eccentricity damping time scale if Eq. 1 is correct. This means that tides will not take over the eccentricity damping until after the migration has essentially stopped.

After migration has stopped, we assumed that the dissipation in Io is reducing its eccentricity on the same time scale as disk interaction did during the migration ($\sim 6.7 \times 10^5$ years)

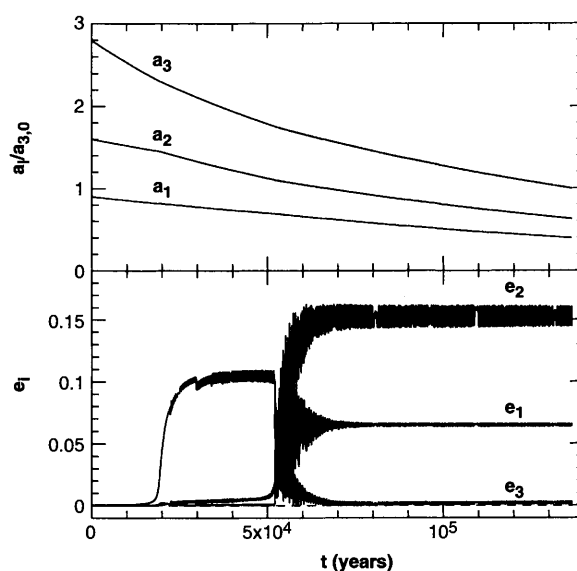


Fig. 1. Nebula-induced evolution of Galilean satellites into the Laplace resonance. The semimajor axes are normalized by Ganymede's current distance from Jupiter $a_{3,0}$. The imposed inward migration and eccentricity damping time scales are $|a_3/\dot{a}_3| \approx 10^5$ years, $|a_1/\dot{a}_1| = |a_2/\dot{a}_2| \approx 2 \times 10^5$ years, and $|e_i/\dot{e}_i| = |a_i/(30\dot{a}_i)|$ $i = 1, 2,$ and 3 . Circular coplanar orbits are assumed initially.

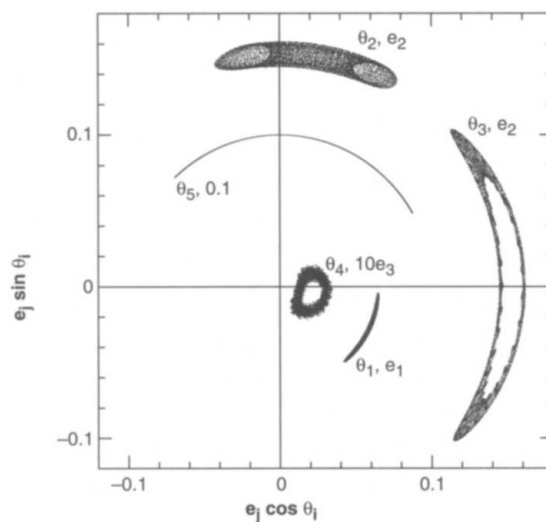


Fig. 2. Libration of 2:1 mean motion resonance variables and the Laplace angle for the asymptotic state of the resonant Galilean satellite configuration shown in Fig. 1. The θ_i are defined in the text. The coefficients e_i , corresponding to the θ_i , are indicated in the figure. Librations are shown for 250 years with all migration and damping removed.

REPORTS

(Figs. 3 and 4). We maintained this time scale for the damping calculation to keep the computer time within reasonable bounds. The algorithm is such that forces are applied to Io that would cause the assumed eccentricity damping if Io were isolated but, because it must drag down the eccentricities of all the satellites locked in the resonances, the actual time scale is much longer. The system naturally relaxes to the current configuration through a series of states with offset libration centers, much like Greenberg described (4). The eccentricities at the end of the calculation have almost reached the values observed currently, and the libration centers have migrated to the current geometry from their positions at the end of migration (Fig. 2)—even to the detail that θ_4 has ended up circulating just as we observe now.

The eccentricity of Ganymede, e_3 , evolves in an interesting way in conjunction with the behavior of θ_4 (Figs. 3 and 4). Initially, the center of libration of θ_4 shifts from near -10° to near 180° in about 10^4 years while e_3 decreases. At 1.5×10^4 years, a sudden jump in e_3 , perhaps from an encounter with a secondary resonance (35), results in θ_4 changing to circulation (angle increasing or decreasing without bound) where it remains until $t = 5 \times 10^4$ years. Here e_3 suddenly becomes smaller, perhaps from another change in the effect of the secondary resonance, and θ_4 again librates about 180° . After $\sim 10^4$ years, θ_4 switches from libration to permanent circulation due to the slow reduction in the forced eccentricity while the free eccentricity remains near 0.0016. In another calculation with a different migration rate, the resonance variable θ_4 shows similar behavior but without the sudden changes in e_3 and with different timing of events. In both cases, θ_4 ends up circulating with $e_3 \approx 0.0016$. This is about the current value of Ganymede's free eccentricity, but there may be circumstances where less excitation of the free eccentricity leaves θ_4 librating.

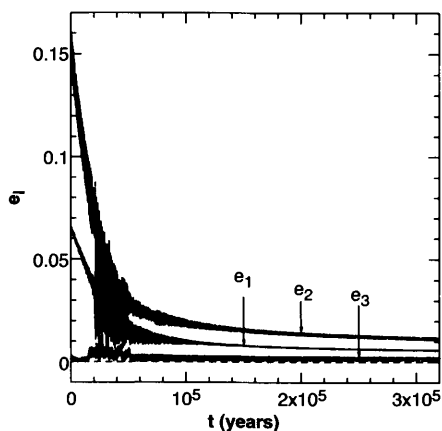


Fig. 3. Relaxation of Galilean satellite system to the current configuration with migration halted and with eccentricity damping in Io alone to simulate the effects of tidal dissipation.

A primordial origin of the Laplace relation relieves Jupiter of providing sufficient tidal torque over history to expand the orbits enough for the completely tidal origin. However, it has been argued that even if the origin of the resonances is primordial, the average Q_j cannot be far from the bounds $6 \times 10^4 \leq Q_j \leq 2 \times 10^6$ established by (1, 2, 4, 11, 36). The current dissipation in Jupiter must still be sufficient to prevent the destruction of the resonances from the tidal dissipation in Io and might be sufficiently high to preserve the system in equilibrium (2, 11). In contrast, could it be that we are witnessing the further decay of the Laplace resonance due to the dissipation in Io (3, 4)? Because the energy dissipated must come from the orbits, a continuing decay of the Laplace configuration would result in an increasing n_1 . Measures of $\dot{n}_1 = \dot{\lambda}_1$, based on 300 years of precise ephemerides of the Galilean satellites coupled with current precise observations, imply either an acceleration of Io's mean motion, indicating further decay of the resonant configuration (37, 38), or insufficient deceleration (39) from Jupiter torques on Io to accommodate the high heat flux from Io in an equilibrium eccentricity configuration. The heat flux is now estimated to be about 3 W/m^2 (40). Although the measurements of \dot{n}_1 remain controversial, we should keep in mind that a heat flux from Io of 3 W/m^2 would require a current $Q_j \approx 2 \times 10^4$ to maintain the system in equilibrium, which is a factor of 3 lower than the minimum historical average $Q_j = 6 \times 10^4$ from the proximity of Io to Jupiter (36). But there is no reason to believe that the current Q_j should be constrained much by a bound on its historical average (6).

A primordial origin of the Laplace relation among the Galilean satellites, created by differential migration of the satellites in the gaseous disk, with the help of tidal dissipation, reproduces every detail of the current configuration.

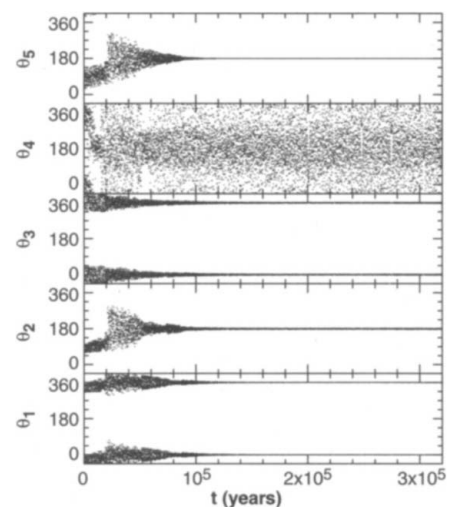


Fig. 4. Behavior of resonance variables for the evolution described in Fig. 3.

Changing assumptions will change details of this scenario such as the asymptotic values of the eccentricities during the migration; a different damping rate may change the circulation of θ_4 . But as long as the satellites exist simultaneously in the disk and the more rapid migration of Ganymede forces the inner-three orbits to converge and capture into the Laplace resonance results (41), the qualitative features of this alternative early history will persist.

References and Notes

1. C. F. Yoder, *Nature* **279**, 767 (1979).
2. ———, S. J. Peale, *Icarus* **47**, 1 (1981).
3. R. Greenberg, in *Satellites of Jupiter*, D. Morrison, Ed. (Univ. Arizona Press, Tucson, AZ, 1982), pp. 65–92.
4. R. Greenberg, *Icarus* **70**, 334 (1987).
5. Free and forced eccentricities are often referred to in discussions of eccentricity type orbital resonances at commensurabilities of the mean motions. In a lowest order eccentricity type resonance between two satellites, where for example the resonance variable $\lambda_1 - 2\lambda_2 + \varpi_1$ is librating about 0° ($n_1 - 2n_2 + \langle \dot{\varpi}_1 \rangle = 0$ on average), conjunctions must occur when satellite 1 is near its periape for stability. This imposes the constraint $\langle \dot{\varpi}_1 \rangle = -(n_1 - 2n_2)$, where the angled brackets denote averaged values. Because $\langle \dot{\varpi}_1 \rangle$ depends on the magnitude of the eccentricity e_1 , the resonant interaction will force e_1 to the appropriate value to accommodate the resonance. If there is a nonzero libration amplitude, the eccentricity will fluctuate about the forced mean value. The magnitude of the fluctuation in e_1 is called the free eccentricity, which can be damped to zero.
6. S. J. Peale, *Annu. Rev. Astron. Astrophys.* **37**, 533 (1999).
7. R. Malhotra, *Icarus* **94**, 399 (1991).
8. A. P. Showman, R. Malhotra, *Icarus* **127**, 93 (1997).
9. A. P. Showman, D. J. Stevenson, R. Malhotra, *Icarus* **129**, 367 (1997).
10. G. W. Ojakangas, D. J. Stevenson, *Icarus* **66**, 341 (1986).
11. S. J. Peale, R. Greenberg, *Lunar Planet. Sci.* **XI**, 871 (1980).
12. J. B. Pollack, J. I. Lunine, W. C. Tittmore, in *Uranus*, J. T. Bergstrahl, E. D. Miner, M. S. Matthews, Eds. (Univ. Arizona Press, Tucson, AZ, 1991), pp. 469–512.
13. G. Schubert, T. Spohn, R. T. Reynolds, in *Satellites*, J. A. Burns, M. S. Matthews, Eds. (Univ. Arizona Press, Tucson, AZ, 1986), pp. 224–292.
14. J. D. Anderson et al., *Science* **281**, 2019 (1998).
15. J. D. Anderson et al., *Science* **280**, 1573 (1998).
16. J. D. Anderson et al., *Icarus* **153**, 157 (2001).
17. D. J. Stevenson, A. W. Harris, J. I. Lunine, in *Satellites*, J. A. Burns, M. S. Matthews, Eds. (Univ. Arizona Press, Tucson, AZ, 1986), pp. 39–88.
18. D. J. Stevenson, *Science* **294**, 71 (2001).
19. R. M. Canup, W. R. Ward, *Astron. J.*, in press.
20. W. R. Ward, J. M. Hahn, in *Protostars and Planets IV*, V. Mannings, A. P. Boss, S. S. Russell, Eds. (Univ. Arizona Press, Tucson, AZ, 2000), pp. 1135–1158.
21. S. H. Lubow, M. Seibert, P. Artymowicz, *Astrophys. J.* **526**, 1001 (1999).
22. G. Bryden, X. Chen, D. N. C. Lin, R. P. Nelson, J. C. B. Papaloizou, *Astrophys. J.* **514**, 344 (1999).
23. W. Kley, G. D'Angelo, T. Henning, *Astrophys. J.* **547**, 457 (2001).
24. G. D'Angelo, T. Henning, W. Kley, *Astron. Astrophys.* **385**, 647 (2002).
25. W. R. Ward, *Icarus* **126**, 261 (1997).
26. Lee and Peale (29) have shown that capture into the resonances at the 2:1 commensurability during differential migration of the two planets in coplanar orbits about the star GJ 876 occurs easily for a reasonably wide range of initial conditions. Capture and subsequent configuration are independent of the migration rate unless that rate is unreasonably large, and the capture and configuration are independent of the functional dependence of the migration on orbital semimajor axes. The only thing that matters is that the orbits converge.

REPORTS

27. J. Wisdom, M. Holman, *Astron. J.* **102**, 1528 (1991).
28. H. F. Levison, M. J. Duncan, *Icarus* **108**, 18 (1944). Available at: www.boulder.swri.edu/~hal/swift.html.
29. M. H. Lee, S. J. Peale, *Astrophys. J.* **567**, 596 (2002).
30. We have arbitrarily assigned the full masses to the satellites and assumed that Io and Europa migrate on the same time scale to demonstrate the hypothesis, whereas migration will ensue as the satellites are accreting and Io will generally migrate faster than Europa once its mass exceeds that of the latter. The necessary condition here for the success of the establishment of the Laplace relation is that Io migrate more slowly than Europa after Europa is captured into resonance with Ganymede, which capture accelerates Europa's migration. The migration rate history thus depends on the surface mass density of the disk and the accretion history determining the satellite masses as a function of time. There is enough flexibility in the disk and accretion model to effect the necessary relative rates.
31. P. Artymowicz, *Astrophys. J.* **419**, 166 (1993).
32. H. Tanaka, T. Takeuchi, W. R. Ward, *Astrophys. J.* **565**, 1257 (2002).
33. S. J. Peale, P. Cassen, R. T. Reynolds, *Icarus* **43**, 65 (1980).
34. ———, *Science* **203**, 892 (1979).
35. W. C. Tittermore, J. Wisdom, *Icarus* **78**, 63 (1989).
36. P. Goldreich, S. Soter, *Icarus* **5**, 375 (1966).
37. S. J. Goldstein, K. C. Jacobs, *Astron. J.* **110**, 3054 (1995).
38. K. Aksnes, F. A. Franklin, *Astron. J.* **122**, 2734 (2001).
39. J. H. Lieske, *Astron. Astrophys.* **176**, 146 (1987).
40. G. J. Veeder, D. L. Matson, T. V. Johnson, A. G. Davies, D. L. Blaney, *AGU Spring Meeting 2002*, 28 to 31 May 2002, Washington, DC (American Geophysical Union, Washington, DC, 2002). Available at: www.agu.org/dbasetop.html.
41. The establishment of the Laplace relation is not a certain outcome for differential migration of the satellites, although some type of resonance configuration does seem certain. Minor changes in the initial conditions, migration rates, or eccentricity damping rates sometimes led to other configurations. For example, in one case the system ended up with Ganymede-Europa in 2:1 resonances and Europa-Io in 7:3 resonances. Accretion of the satellites may not have been complete at the time of capture into the resonances, but two identical calculations—one with the full satellite masses and the other with half these masses—led to very similar Laplace configurations. Even if the mass ratios vary during migration, the configuration at the end of migration should be the same. The conditions for the various end configurations and an estimate of the probability of the system selecting the Laplace configuration will be subjects of a future paper.
42. We thank R. Canup and W. Ward for sending us an early preprint of their paper on Galilean satellite origin. This research was supported in part by NASA PGC grants NAG5 3646 and NAG5 11666 and SSO grants NAG5 7177 and NAG5 12087.

25 July 2002; accepted 16 September 2002

"Stemness": Transcriptional Profiling of Embryonic and Adult Stem Cells

Miguel Ramalho-Santos,¹ Soonsang Yoon,² Yumi Matsuzaki,² Richard C. Mulligan,² Douglas A. Melton^{1*}

The transcriptional profiles of mouse embryonic, neural, and hematopoietic stem cells were compared to define a genetic program for stem cells. A total of 216 genes are enriched in all three types of stem cells, and several of these genes are clustered in the genome. When compared to differentiated cell types, stem cells express a significantly higher number of genes (represented by expressed sequence tags) whose functions are unknown. Embryonic and neural stem cells have many similarities at the transcriptional level. These results provide a foundation for a more detailed understanding of stem cell biology.

Stem cells (SCs) have the capacity to self-renew as well as the ability to generate differentiated cells. Recently, the field of SC biology has attracted increasing attention because of the isolation of human embryonic SCs (1, 2) and the suggestion that adult SCs may have a broader potential or plasticity than was previously thought [(3), reviewed in (4), but see (5, 6)]. Understanding the genes that govern the special properties of SCs has implications for both embryology and basic cell biology. Despite this interest and the potential for use of SCs in cell replacement therapy, relatively little is known about the genetic programs for SCs.

The three best characterized types of SCs in vertebrates are embryonic (ESC), neural (NSC), and hematopoietic (HSC) stem cells. There is indirect evidence for SCs in intestine,

skin, muscle, and liver, but their isolation has remained elusive (4, 7). Few genes are known to play roles in SCs or to be useful for SC isolation (4, 7). Genes expressed in ESCs have been identified with cDNA arrays containing ~600 genes (8), and genes enriched in NSCs (9) or HSCs (10, 11) have been identified by subtractive hybridization. However, many genes expected to be enriched in SCs were not identified by these methods (12), and the use of different methods precludes a direct comparison of results from different stem cells (8–11).

We established transcriptional profiles for ESCs, NSCs, HSCs, and the differentiated cells from lateral ventricles of the brain and from the main cell population of the bone marrow (Fig. 1). This protocol is intended to first identify genes enriched in each individual stem cell population and then compare those sets of genes to one another. The methodological details (12) can be summarized as follows. Replicates of mouse stem and differentiated cell samples were isolated, and amplified probes were prepared by *in vitro* transcription and then hybridized to DNA microarrays (Affymetrix U74Av2) containing about 12,000 genes. Scanned arrays were analyzed with Affymetrix

MAS 4.0 software to identify transcripts absent in differentiated cells but present in SCs, and with dChip software, a statistical method for model-based expression analysis (13), to obtain expression indices that identify transcripts enriched in SCs. In each comparison, a 90% confidence interval was calculated for the fold change in gene expression, and the lower limit of this interval—the lower confidence bound (LCB)—was used as a measure of enrichment in gene expression. Li and Wong (14) have shown that the LCB is more reliable than fold change as a ranking statistic for changes in gene expression. Yuen *et al.* (15) compared data from Affymetrix chips and real-time polymerase chain reaction and concluded that chip analyses are accurate, reliable, and underestimate differences in gene expression. In view of their work, our criterion of selecting genes with LCBs above 1.2 (which corresponds to an estimated fold change of 1.9 in gene expression) most likely corresponds to a fold change of at least 3 in gene expression. The reproducibility of our results is underscored by the high correlation coefficients of the replicates (which have a mean of 0.98 and a range of 0.96 to 1.00); 7786 genes, 63% of the array, were reproducibly detected (called "present"), indicating that a substantial portion of the mouse genome was assayed.

Lateral ventricles of the brain and the main cell population of the bone marrow were used as baselines for NSCs and HSCs, respectively, as they correspond to differentiated cell types for these SCs. For ESCs, which give rise to all mouse cell types, we compared them to lateral ventricles of the brain and the main cell population of the bone marrow and then intersected the comparisons (i.e., we selected only genes that showed a significant enrichment in both comparisons). This method proved to be effective for detecting genes expected from the literature to be enriched in ESCs (Fig. 1). Genes enriched in ESCs, NSCs, and HSCs were assigned to functional categories with the use of NetAffx.com and National Center for Biotech-

¹Department of Molecular and Cellular Biology and Howard Hughes Medical Institute (HHMI), Harvard University, Cambridge, MA 02138, USA. ²Department of Genetics, Harvard Medical School, Boston, MA 02115, USA.

*To whom correspondence should be addressed. E-mail: dmelton@mcb.harvard.edu